AMERICAN SOCIETY FOR MICROBIOLOGY | mBio®

RESEARCH ARTICLE
Molecular Biology and Physiology

Regulation of Iron Storage by CsrA Supports Exponential Growth of *Escherichia coli*

Christine Pourciau,[a] Archana Pannuri,[a] Anastasia Potts,[a]* Helen Yakhnin,[b] Paul Babitzke,[b] Tony Romeo[a]

[a]Department of Microbiology and Cell Science, Institute of Food and Agricultural Sciences, University of Florida, Gainesville, Florida, USA
[b]Department of Biochemistry and Molecular Biology, Center for RNA Molecular Biology, The Pennsylvania State University, University Park, Pennsylvania, USA

ABSTRACT The global regulatory protein CsrA coordinates gene expression in response to physiological cues reflecting cellular stress and nutrition. CsrA binding to the 5′ segments of mRNA targets affects their translation, RNA stability, and/or transcript elongation. Recent studies identified probable mRNA targets of CsrA that are involved in iron uptake and storage in *Escherichia coli*, suggesting an unexplored role for CsrA in regulating iron homeostasis. Here, we assessed the impact of CsrA on iron-related gene expression, cellular iron, and growth under various iron levels. We investigated five new targets of CsrA regulation, including the genes for 4 ferritin or ferritin-like iron storage proteins (ISPs) and the stress-inducible Fe-S repair protein, SufA. CsrA bound with high affinity and specificity to *ftnB, bfr*, and *dps* mRNAs and inhibited their translation, while it modestly activated *ftnA* expression. Furthermore, CsrA was found to regulate cellular iron levels and support growth by repressing the expression of genes for ISPs, most importantly, ferritin B (FtnB) and bacterioferritin (Bfr). Iron starvation did not substantially affect cellular levels of CsrA or its small RNA (sRNA) antagonists, CsrB and CsrC. *csrA* disruption led to increased resistance to the lethal effects of H_2O_2 during exponential growth, consistent with a regulatory role in oxidative stress resistance. We propose that during exponential growth and under minimal stress, CsrA represses the deleterious expression of the ISPs that function under oxidative stress and stationary-phase conditions (FtnB, Bfr, and Dps), thus ensuring that cellular iron is available to processes that are required for growth.

IMPORTANCE Iron is an essential micronutrient for nearly all living organisms but is toxic in excess. Consequently, the maintenance of iron homeostasis is a critical biological process, and the genes involved in this function are tightly regulated. Here, we explored a new role for the bacterial RNA binding protein CsrA in the regulation of iron homeostasis. CsrA was shown to be a key regulator of iron storage genes in *Escherichia coli*, with consequential effects on cellular iron levels and growth. Our findings establish a model in which robust CsrA activity during the exponential phase of growth leads to repression of genes whose products sequester iron or divert it to unnecessary stress response processes. In so doing, CsrA supports *E. coli* growth under iron-limiting laboratory conditions and may promote fitness in the competitive iron-limited environment of the host large intestine.

KEYWORDS CsrA, CsrB, CsrC, RNA binding proteins, bacterial growth, ferritin, iron homeostasis, iron storage proteins, oxidative stress, posttranscriptional regulation, sRNAs, stress responses

Bacteria such as *Escherichia coli* have evolved complex and efficient global regulatory systems that enable them to recognize and adapt to changing environmental conditions, thus supporting their growth, survival, competition, and host-microbe interactions. The carbon storage regulatory system (Csr) is one such system and plays

Citation Pourciau C, Pannuri A, Potts A, Yakhnin H, Babitzke P, Romeo T. 2019. Regulation of iron storage by CsrA supports exponential growth of *Escherichia coli*. mBio 10:e01034-19. https://doi.org/10.1128/mBio.01034-19.

Editor Bonnie Bassler, Princeton University

Address correspondence to Tony Romeo, tromeo@ufl.edu.

* Present address: Anastasia Potts, Takara Bio USA, Inc., Mountain View, California, USA.

Received 23 April 2019
Accepted 8 July 2019
Published 6 August 2019

a critical a role in controlling numerous important cellular processes, including central carbon metabolism (1–3), stress response systems (4–6), biofilm formation (7), motility (8), quorum sensing (9), and virulence properties of pathogens (10). The Csr system is widely distributed among bacteria, with homologous regulatory factors sometimes referred to as Rsm (repressor of secondary metabolites) (11, 12).

The key component of the Csr system is CsrA, a homodimeric, sequence-specific RNA-binding protein, encoded by *csrA* (13–15). In general, CsrA represses the expression of genes associated with stress responses and stationary-phase growth (4, 16), while activating the expression of genes that support exponential growth (16, 17). CsrA binds to mRNA targets at sites containing a GGA motif surrounded by semiconserved sequences, with the GGA often located in the single-stranded loop of a hairpin (18, 19). The binding of CsrA to sites located in the 5′ untranslated region (5′ UTR) or the early coding region can result in altered translation (20–23), altered RNA stability (8, 24), and/or changes in RNA secondary structure that affect Rho-dependent transcription termination (25).

CsrA itself is subject to multifaceted regulation (16). While *csrA* gene expression is regulated transcriptionally and posttranscriptionally (26), CsrA activity is controlled by the small RNAs (sRNAs) CsrB and CsrC. These sRNAs contain multiple high-affinity binding sites that mimic those of target mRNAs, allowing CsrB/C to bind to and sequester many CsrA dimers (27). CsrB and CsrC transcription is activated by amino acid limitation or other stresses via ppGpp/DksA (4), metabolic end products, e.g., acetate and formate, via BarA-UvrY (12, 28), and extracytoplasmic stress via σ^E (6). Their RNase E-mediated turnover is triggered by glucose, via interaction of $EIIA^{glc}$ with CsrD (29–31). Thus, CsrB/C sRNAs accumulate and sequester CsrA when preferred carbon resources have been expended, amino acids are limiting, metabolic end products have accumulated, and/or cells experience extracellular stress. Antagonism of CsrA by CsrB/C promotes the transition from glycolytic metabolism and active growth to gluconeogenesis, glycogen biosynthesis, and the formation of a stress-resistant phenotype (30).

A recent transcriptomics analysis in *E. coli* revealed that CsrA affects the expression of numerous genes involved in iron uptake and metabolism and confirmed its effects on levels of four such mRNAs (19). Several of the genes were of particular interest due to their importance in iron homeostasis and/or the large magnitude of CsrA effects (19). These effects of CsrA were suspected of occurring indirectly, as they were not confirmed by *in vivo* binding of CsrA to the mRNAs using cross-linking immunoprecipitation sequencing (CLIP-seq). However, CLIP-seq analyses have constraints, sources of bias (32), and are limited in sensitivity (33), potentially generating false-negative results.

Iron is an essential micronutrient for nearly all living organisms and required for fundamental processes such as respiration, central metabolism, genetic regulation, and DNA repair (34). It is the most common transition metal found in proteins, typically within heme or Fe-S prosthetic groups (35, 36). Although iron is abundant in many environments, ferric iron (Fe^{3+}) predominates under aerobic conditions at neutral pH. Fe^{3+} has poor aqueous solubility and exists as insoluble salts and oxides or bound to host iron-binding proteins (37). Soluble ferrous iron (Fe^{2+}) is biologically available but is rapidly oxidized to ferric iron at neutral or higher pH under aerobic conditions (35). Consequently, microbes have evolved high-affinity acquisition systems to scavenge iron (38). An added complication is that Fe^{2+} can be cytotoxic due to its role in producing damaging hydroxyl radicals ($^{\cdot}OH$) from H_2O_2 via the Fenton reaction. Thus, free intracellular iron levels are tightly controlled (34, 39). Additionally, iron availability can serve as an important cue regarding the environment of the bacterium, affecting virulence processes in many pathogens (38, 40).

Intracellular iron storage proteins (ISPs) sequester iron, providing iron reserves and protection against toxicity (35). Three related classes of bacterial ISPs exist: archetypal ferritins, heme-containing bacterioferritins, and Dps proteins (DNA protection during starvation). Each of these proteins is composed of identical subunits that form a roughly spherical shell surrounding a central cavity that acts as an iron storage reservoir (34). Ferritins and bacterioferritins are composed of 24 subunits and can accommodate

2,000 to 3,000 iron ions; Dps proteins have 12 subunits and can store ~500 iron ions (34). A key feature of ISPs is the ferroxidase center, which binds two ferrous ions and oxidizes them using molecular oxygen or H_2O_2, forming a diferric intermediate that migrates to the central core for storage (35). Bacteria often possess multiple ferritin or bacterioferritin genes (34). *E. coli* expresses two ferritins (FtnA and FtnB), one bacterioferritin (Bfr), and one Dps.

Assembly of the iron-sulfur (Fe-S) clusters that serve as cofactors for enzymes is a crucial biological function, performed by Fe-S biogenesis systems (41, 42). In *E. coli*, most Fe-S cluster formation under nonstress conditions is by the "housekeeping" Isc pathway, encoded by the *iscRSUA-hscBA-fdx* (*isc*) operon (42, 43). Alternatively, the Suf pathway, encoded by the *sufABCDSE* (*suf*) operon, is more robust than Isc against oxidative damage and is favored for Fe-S assembly during oxidative and nitrosative stress or when iron is limiting (44–47). The coordinated regulation of these pathways accommodates the changing requirements for Fe-S cluster biogenesis, which fluctuate with growth conditions (43, 48).

In *E. coli* and most bacteria, the DNA-binding ferric uptake regulator protein, Fur, controls iron metabolism (49). Fur activity depends on cellular free iron, which acts as a corepressor of transcription (40). Fur also activates gene expression via RNA polymerase recruitment, blocking repressor access, or transcriptional repression of RyhB sRNA (36). RyhB base pairing stimulates the degradation of mRNAs encoding nonessential iron-dependent proteins, increasing iron availability for essential processes (50). The goal of the present study was to explore the effects of CsrA on *E. coli* iron homeostasis. Unlike Fur and RyhB, we show that CsrA is not responsive to iron availability but nevertheless exerts biologically important effects on iron homeostasis and growth by regulating the expression of ISPs.

RESULTS

CsrA regulates expression of iron storage genes independently of Fur. Recent transcriptomics and other studies identified several potential mRNA targets of CsrA-mediated regulation that are involved in iron uptake and storage, suggestive of a regulatory role in iron metabolism (4, 19, 51). To further investigate this possibility, twelve of these genes were chosen for expression analysis (see Table S1 in the supplemental material). Altogether, eleven translational *'lacZ* fusions and one C-terminal 3×FLAG-tagged reporter fusion were constructed and integrated in single copy into the *E. coli* chromosome.

We assessed the expression of the following genes, which encode the indicated proteins. We assessed four iron transport genes: (i) *fhuE*, an outer membrane receptor for the xenosiderophores coprogen, ferrioxamine B, and rhodotorulic acid; (ii) *fecB*, the periplasmic ferric-citrate transporter; (iii) *fepA*, the ferrienterobactin outer membrane receptor; and (iv) *fhuA*, the outer membrane transporter for ferrichrome. Four genes encoding ISPs were assessed: (i) *ftnA*, the primary reservoir for iron in *E. coli* K-12; (ii) *ftnB*, a ferritin-like ISP; (iii) *bfr*, a heme-sequestering bacterioferritin; and (iv) *dps*, an iron-sequestering and nonspecific DNA-binding protein that protects DNA in starved cells. Two genes related to siderophores were investigated: (i) *fes*, enterobactin esterase, which hydrolyzes the siderophore backbone to release bound iron; and (ii) *entC*, an isochorismate synthase involved in enterobactin biosynthesis. Lastly, the genes encoding Fur and an Fe-S cluster assembly protein, SufA, were examined.

Expression of the reporter fusions was monitored in the wild-type (WT) strain background MG1655 and in isogenic *csrA*, *fur*, and *csrA fur* mutant strains. These studies confirmed CsrA-dependent regulation of five iron metabolism genes (Fig. 1A to E). Translational fusions for three iron storage genes (*ftnB*, *bfr*, and *dps*) were strongly repressed by CsrA (Fig. 1A to C). The *ftnB'-'lacZ* fusion exhibited the most striking effect, with a 14-fold increase in the *csrA* mutant. Fur did not affect *ftnB'-'lacZ* expression under the conditions of this study (Fig. 1A). Expression of *bfr'-'lacZ* increased 7-fold in the *csrA* mutant (Fig. 1B). The *bfr* gene has been reported to be posttranscriptionally regulated by the Hfq-dependent sRNA RyhB, which is repressed by Fur (52). In contrast,

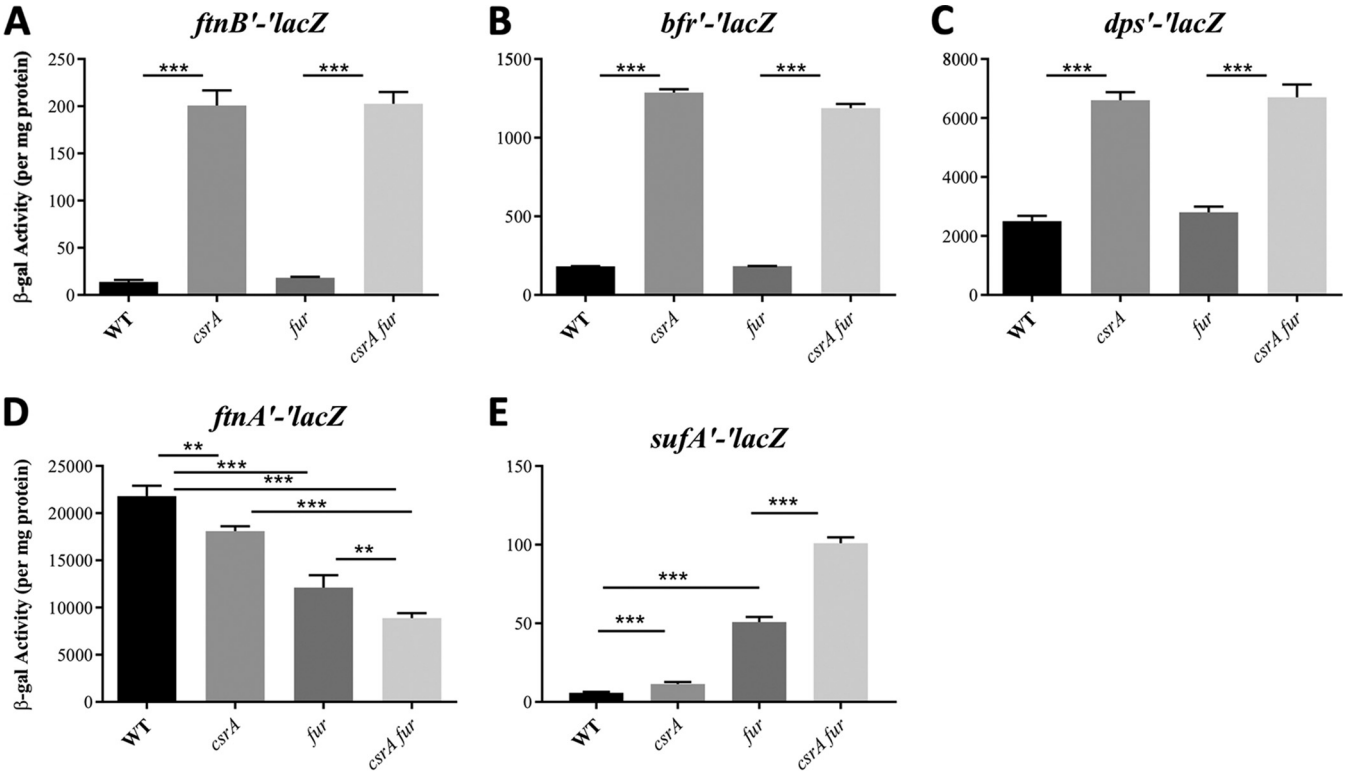

FIG 1 (A to E) Effects of *csrA* and *fur* mutations on expression of translational *lacZ* fusions. Mean β-galactosidase activities $\pm$ standard deviation were determined from exponential-phase cultures (OD_{600} of 0.5) grown in LB. Each bar shows the mean and standard deviation from four separate experiments. Statistical significance was determined using unpaired *t* tests and denoted as follows: ***, $P < 0.001$; **, $P < 0.002$.

we did not observe Fur-dependent regulation of the *bfr*′-′*lacZ* fusion. As the RyhB binding site in *bfr* mRNA has yet to be identified, it is conceivable that our fusion did not encompass that region. Finally, an ~3-fold increase in the *csrA* mutant was observed for *dps*′-′*lacZ*, which did not respond to Fur (Fig. 1C).

Moderate CsrA-dependent effects were observed for *ftnA* and *sufA* fusions (Fig. 1D and E). The *ftnA*′-′*lacZ* showed positive effects of CsrA on its expression, which were retained in the Δ*fur* mutant (Fig. 1D). Thus, CsrA has a minor role in activating *ftnA* gene expression that is mediated independently of Fur. The *sufA*′-′*lacZ* fusion exhibited modest repression via CsrA in the *fur* WT and mutant backgrounds (Fig. 1E). The *entC*, *fhuE*, *fepA*, *fes*, and *fhuA* translational fusions were all repressed by Fur but were not regulated by CsrA (Fig. S1A to E). Expression of *fur*′-′*lacZ* was unaffected by CsrA (Fig. S1F). Altogether, these findings demonstrate that CsrA effects on iron-related gene expression are mediated independently of Fur.

Growth phase-dependent regulation of *ftnB, bfr,* and *dps* expression by CsrA. Having identified three iron storage genes, *ftnB*, *bfr* and *dps*, that are repressed by CsrA, we assessed their expression during exponential phase, the transition from exponential to stationary phase, and stationary-phase growth at 24 h. Complementation tests were performed using plasmid-borne *csrA* (pCRA16) versus the empty vector (pBR322). The *ftnB*, *dps*, and *bfr* fusions all exhibited growth phase-dependent regulation by CsrA, which was abolished by complementation (Fig. 2). CsrA repressed the three genes maximally during exponential growth, with weaker effects in the transition to stationary phase and in stationary phase. The *bfr* and *dps* fusions were not regulated by CsrA during stationary phase (Fig. 2B and C), while *ftnB* repression decreased from 14-fold in the exponential phase to ~4-fold at 24 h (Fig. 2A). *ftnB* expression peaked during the transition to stationary phase and remained higher in the *csrA* mutant in all stages of growth (Fig. 2A). *bfr* expression levels were lowest in exponential phase, higher at transition to stationary phase, and then decreased modestly in stationary phase

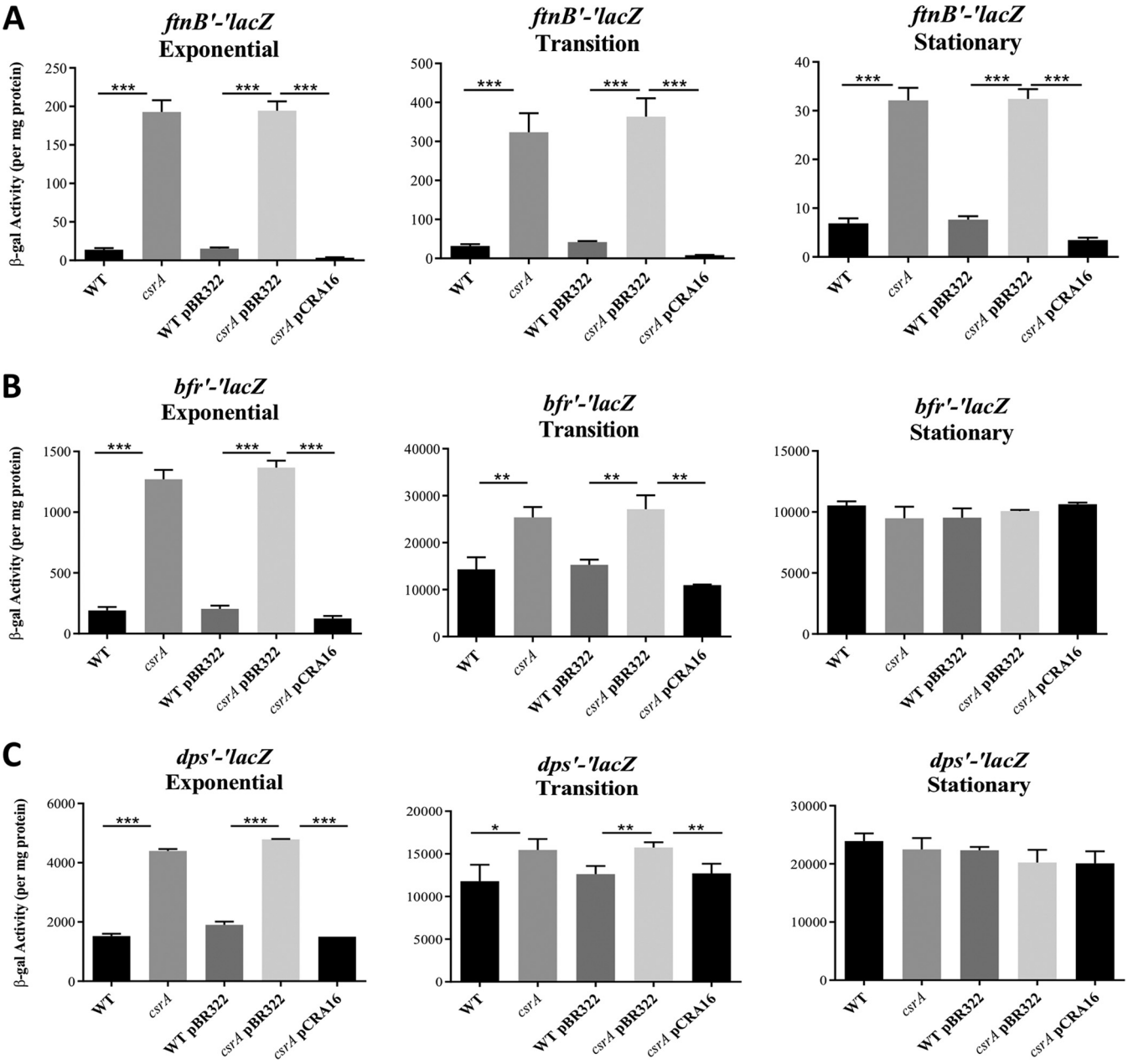

FIG 2 Effects of *csrA* mutation, vector control (pBR322), and *csrA* complementation (pCR16) on expression of the *ftnB* (A), *bfr* (B), and *dps* (C) translational *lacZ* fusions. β-Galactosidase activities $\pm$ standard deviations were determined in exponential-phase (OD_{600} of 0.5), transition to stationary-phase (OD_{600} of 1.5), and overnight cultures grown in LB. Each bar shows the mean and standard deviation from four separate experiments. Statistical significance was determined using unpaired *t* tests and denoted as follows: ***, $P < 0.001$; **, $P < 0.002$; *, $P < 0.05$.

(Fig. 2B). Finally, the growth-phase expression pattern of *dps* reflected what was already known; Dps levels are low during exponential growth and increase upon entry to stationary phase (Fig. 2C) (53). Thus, CsrA plays a particularly important role in limiting the expression of these three genes during exponential growth.

CsrA binds with high affinity and specificity to 5′ UTRs of *ftnB*, *dps*, and *bfr* transcripts. Although a CLIP-seq assay did not identify *in vivo* CsrA binding, previous transcriptomics data demonstrated that CsrA affects the stability and abundance of *ftnB* and *dps* mRNA (19), suggestive of posttranscriptional regulation. To explore the possible binding of CsrA to *ftnB*, *bfr*, and *dps* transcripts, electrophoretic gel mobility shift assays (EMSA) were performed. CsrA exhibited high-affinity binding to all three RNAs (Fig. 3B to D). A nonlinear least-squares analysis of the data yielded apparent K_D

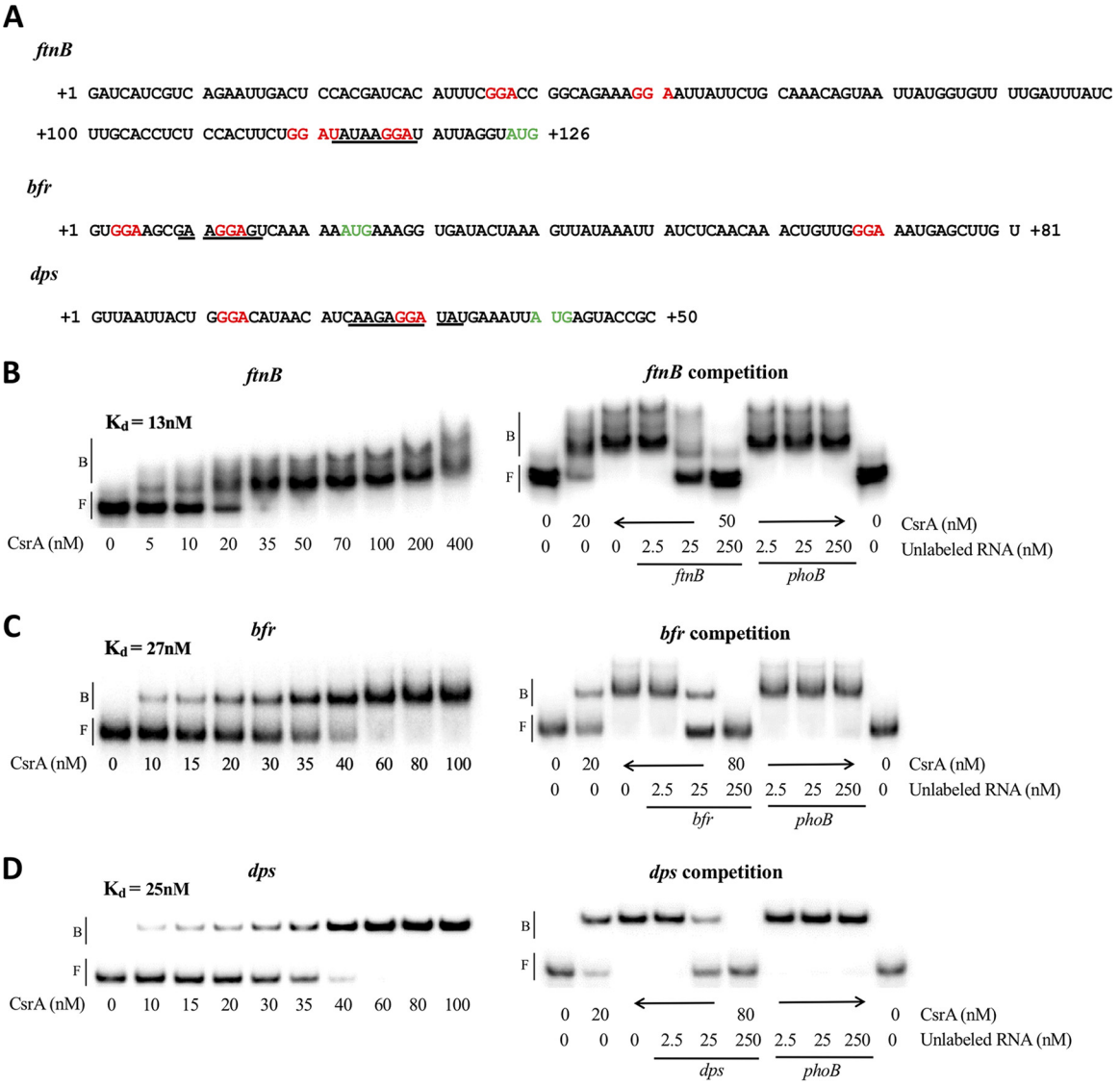

FIG 3 CsrA binding and competition reactions with *ftnB* (B), *bfr* (C), and *dps* (D) transcripts. (A) EMSA probe sequences with GGA sequences that are potential CsrA binding sites shown in red, translation initiation sites in green, and Shine-Dalgarno (SD) sequences underlined. (B to D) 5′-End-labeled transcripts (0.5 nM) were incubated with CsrA at the concentrations shown. Competition reactions were performed in the presence of specific or nonspecific (*phoB*) unlabeled competitor RNAs at the concentrations shown. The positions of free (F) and bound (B) RNA are marked with vertical bars.

(equilibrium binding constant) values of 13 nM, 27 nM, and 25 nM for the *ftnB*, *bfr*, and *dps* RNAs, respectively, similar to those for known CsrA mRNA targets (26, 54). The *bfr* and *dps* mRNAs displayed a single shift as CsrA concentration was raised to 100 nM, while two distinct shifted species and a faint minor form were observed for *ftnB* at 50 nM and higher, suggesting that more than one CsrA dimer may bind to this RNA. Examination of the *ftnB* sequence identified four potential CsrA binding sites, while the *bfr* and *dps* sequences contained three and two potential CsrA binding sites, respectively (Fig. 3A). Competition assays performed with specific (self) and nonspecific (*phoB*) unlabeled competitor transcripts confirmed that binding is specific in all cases (Fig. 3B to D).

Taken together with reporter fusion data (Fig. 1 and 2) and transcriptomics studies (19), the high-affinity binding of CsrA to *ftnB* mRNA suggests that CsrA may directly regulate expression of this gene by binding to its 5′ UTR. CsrA also bound tightly to the 5′ UTR of *dps* mRNA, although the interpretation of this interaction is less clear. While

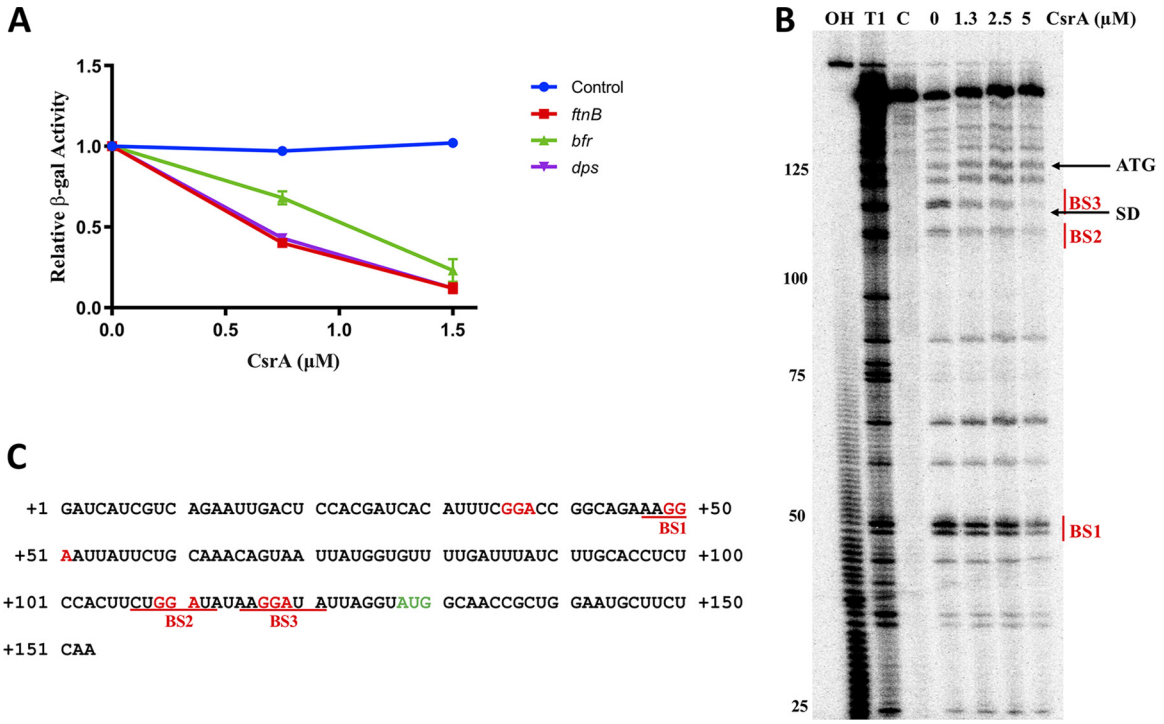

FIG 4 Repression of *ftnB*, *dps*, and *bfr* translation *in vitro* by CsrA and RNase T1 footprinting of *ftnB* RNA. (A) CsrA effects on cell-free protein synthesis of β-galactosidase from plasmid templates containing *′lacZ* fused to the 5′ UTR of each mRNA target and transcribed from a T7 promoter. Relative β-galactosidase activity depicts the mean and standard deviation of activity relative to reaction mixtures lacking CsrA. (B) CsrA-*ftnB* RNA footprint. 5′-End-labeled *ftnB* RNA was treated with RNase T1 ± CsrA, as shown. Partial alkaline hydrolysis (OH) and RNase T1 digestion (T1) ladders, as well as a control lane without treatment (C), are shown. Positions of the *ftnB* start codon (ATG) and the Shine-Dalgarno (SD) sequence are marked. Residues protected from RNase T1 cleavage by CsrA are indicative of binding at three sites, BS1 to -3, and are shown. Numbering is with respect to the start of *ftnB* transcription. (C) Sequence of *ftnB* leader RNA. Position of the translation initiation codon indicated in green, GGA sequences are shown in red, and the deduced CsrA binding sites are indicated.

CsrA negatively affects *dps* RNA abundance and translation (as measured by changes in ribosome occupancy), it increases *dps* mRNA stability (19). It is likely that CsrA binding to the *dps* 5′ UTR is responsible for one or more of these effects. Finally, the high-affinity binding of CsrA to the 5′ UTR of the *bfr* transcript, along with increased mRNA abundance in the *csrA* mutant (19), suggests that CsrA may directly repress *bfr* expression by binding its 5′ UTR.

CsrA directly represses translation of *ftnB*, *dps*, and *bfr* via their 5′ UTRs. To assess whether the regulatory effects of CsrA on *ftnB*, *bfr*, and *dps* are mediated posttranscriptionally, without the requirement for an intermediate regulatory gene, we used the PURExpress system to measure *lacZ* expression from reporter fusions carried on plasmid templates. Reporter sequences contained a T7 promoter fused to the 5′ UTR of each gene and a few codons of the coding region (Fig. 3A). In all cases, with the exception of the control (*pnp′-′lacZ*), expression was inhibited by CsrA. Thus, CsrA represses translation of *ftnB*, *bfr*, and *dps* via their 5′ UTRs (Fig. 4A). The *in vitro* translational repression exhibited by the *dps* reporter was similar to that by the *ftnB* reporter. This pattern of regulation differs from what was seen in the *in vivo* translational fusion assays, where *dps* demonstrated substantially less CsrA-dependent repression than *ftnB* (Fig. 2). This difference may result from increased *dps* mRNA stability, which was observed previously in the *csrA* mutant strain (19), or it might involve indirect effects of CsrA on *dps* transcription *in vivo*.

To identify the precise CsrA interaction site(s) for the most strongly regulated gene, *ftnB*, RNA footprinting experiments were performed. Three regions were protected from RNase T1–mediated cleavage with increasing concentrations of CsrA (Fig. 4B). The protected nucleotides correspond to three of the four GGA motifs, indicating that CsrA has three authentic binding sites in the *ftnB* 5′ UTR (Fig. 4C) (BS1, BS2, and BS3). BS3,

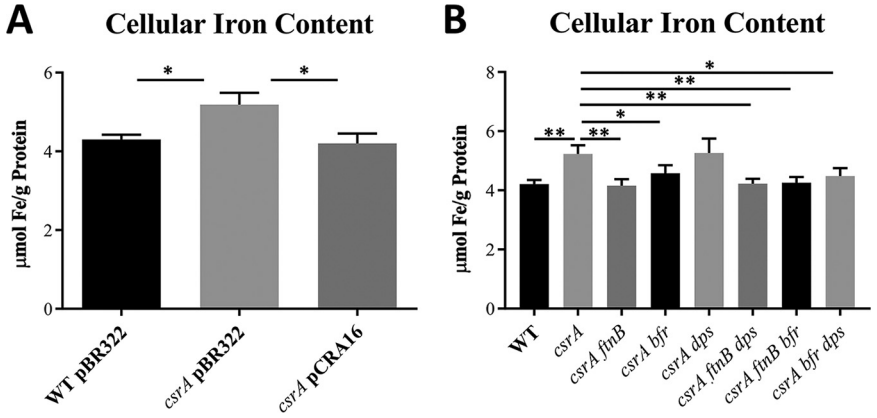

FIG 5 Cellular iron content in *E. coli* strains. Cells were harvested during exponential growth (OD_{600} of 0.5) in LB, lysed with 30% nitric acid, and iron was quantified via ICP-OES. (A) Comparison of iron levels in WT, *csrA* mutant, and *csrA*-complemented strains. (B) Iron content of WT, *csrA*, and combinatorial mutants in genes for iron storage proteins. Each bar shows the mean and standard deviation from two separate biological experiments with paired technical replicates. Statistical significance was determined using unpaired *t* tests and is denoted as follows: **, $P < 0.002$; *, $P < 0.05$.

which overlaps the *ftnB* Shine-Dalgarno (SD) sequence, exhibited the strongest protection by CsrA. This finding provides a molecular mechanism for *ftnB* translational repression by CsrA, observed *in vitro* (Fig. 4A). The multiple protected regions are consistent with EMSA results, which show that more than one complex is formed between CsrA and the *ftnB* 5′ UTR (Fig. 3B).

Overexpression of iron storage genes in the *csrA* mutant increases cellular iron levels. To determine the effect of CsrA regulation of iron storage genes on cellular iron levels, exponential-phase cultures were analyzed for iron content by inductively coupled plasma optical emission spectrometry (ICP-OES). Cellular iron content was ~25% higher in the *csrA* mutant (5.2 ± 0.15 μmol Fe/g protein) than in the WT (4.2 ± 0.07 μmol Fe/g protein) and was restored to the WT level upon complementation (Fig. 5A). This result is consistent with the increased expression of *ftnB*, *bfr*, and *dps* in the *csrA* mutant, which should increase its capacity for iron storage. To test this hypothesis, deletions of the chromosomal *ftnB*, *bfr*, and *dps* genes were introduced, and cellular iron levels were measured. Iron levels in the *csrA* mutant approached WT levels when FtnB and/or Bfr production was abolished (Fig. 5B), suggesting that increased iron accumulation in the *csrA* mutant is caused by the overproduction of these ISPs. The *dps* mutation had no substantial effect on iron levels, alone or in combination with *ftnB* or *bfr*. Notably, the increased iron in the *csrA* mutant may not be biologically available. In fact, excessive iron sequestration by FtnB and Bfr in the *csrA* mutant might inhibit iron-dependent cellular processes, to the detriment of cell growth.

Growth under iron-limiting conditions is compromised by *csrA* mutation and restored by deletion of *ftnB* and *bfr*. To test the above hypothesis, we monitored the growth kinetics of WT, *csrA*, *ftnB*, *bfr*, and/or *dps* mutants under iron-replete and iron-limiting conditions in both rich and minimal media. Growth in rich medium was assessed by tracking total cell protein of cultures grown in LB (for iron-replete conditions) and LB containing 400 μM 2,2′-dipyridyl (DIP) (for iron-limiting conditions). Growth in minimal medium was evaluated by measuring the optical density at 600 nm (OD_{600}) in MOPS (morpholinepropanesulfonic acid) medium supplemented with 100 μM $FeSO_4$ (iron replete) or 0.05 μM $FeSO_4$ (iron limiting) and 0.2% glucose (55). However, biofilm formation compromised growth measurements (A_{600}) in MOPS medium. Under this condition, biofilm was apparently dependent upon the formation of curli fimbriae and was abolished by deletion of *csgA* (data not shown). Thus, all strains examined in MOPS medium were constructed in a *csgA* background.

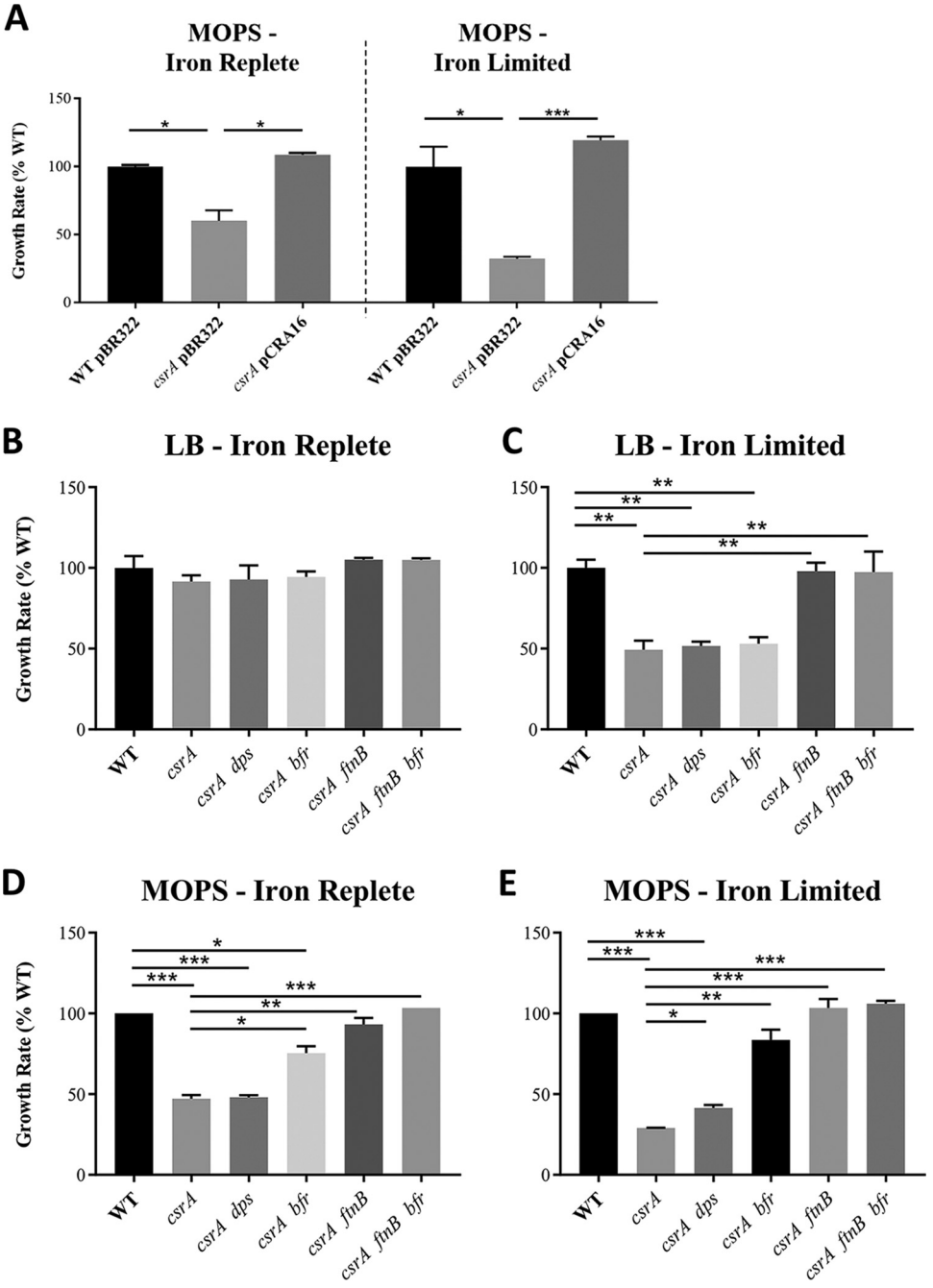

FIG 6 Growth rates (μ) of exponential-phase *E. coli* strains in LB $\pm$ 400 μM DIP and MOPS minimal medium with replete (100 μM) or limiting (0.05 μM) $FeSO_4$ as indicated. (A) WT, *csrA* mutant, and *csrA*-complemented strains in MOPS. (B and C) WT, *csrA* mutant, and *ftnB*/*dps*/*bfr* combinatorial mutants in LB. (D and E) WT, *csrA* mutant, and *ftnB*/*dps*/*bfr* combinatorial mutants in MOPS. Each bar represents the mean and standard deviation from 4 separate experiments. See Fig. S2 in the supplemental material for associated growth curves. Statistical significance was determined using unpaired *t* tests. ***, $P < 0.001$; **, $P < 0.002$; *, $P < 0.05$.

Growth of the WT and *csrA* strains was inhibited under iron-limiting conditions in both media, and these growth defects were particularly severe in the *csrA* mutant (Fig. 6; Fig. S2). To assess the contribution of each iron storage gene to the growth inhibition exhibited by the *csrA* mutant, deletions in the chromosomal *ftnB*, *bfr*, and *dps* genes were introduced into the WT and *csrA* mutant. Each strain was grown under iron-replete and iron-limiting conditions in both the rich (Fig. 6B and C; Fig. S2B and C) and minimal (Fig. 6D and E; Fig. S2D and E) media. The inactivation of *ftnB*, *bfr*, or *dps*

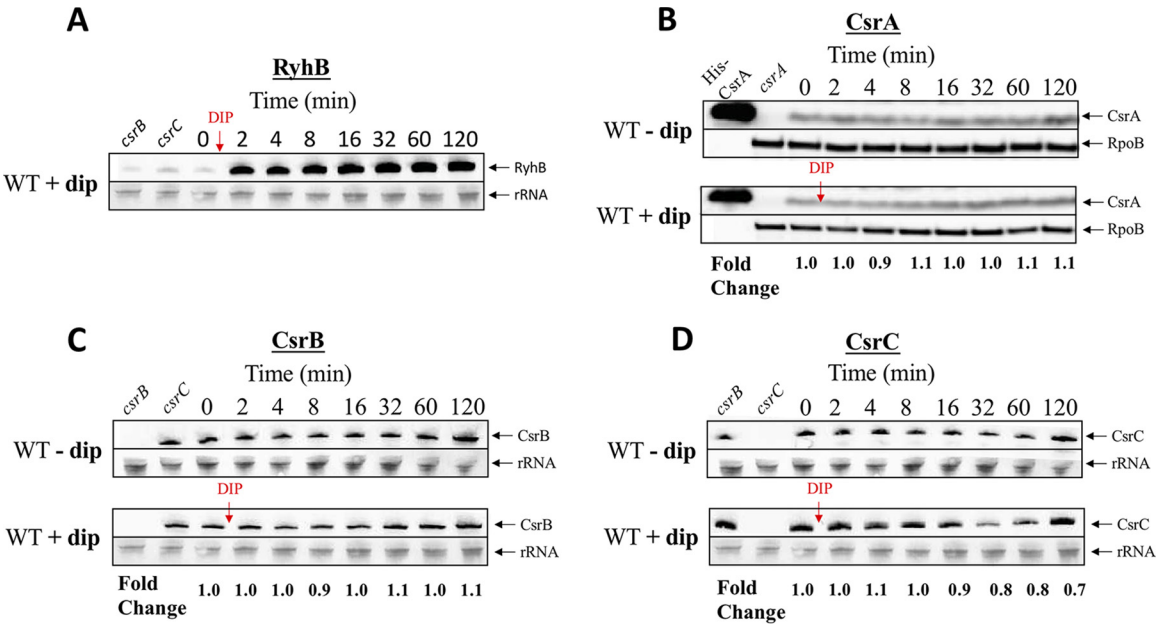

FIG 7 Effects of the addition of 250 μM 2,2′-dipyridyl (DIP) on RyhB (A), CsrA (B), CsrB (C), and CsrC (D) levels at mid-exponential-phase growth (OD_{600} of 0.5). CsrA protein was detected by Western blotting and RyhB and CsrB/C sRNAs were detected by Northern blotting. Values were normalized against RpoB or rRNA, respectively, to calculate specific levels of CsrA, CsrB, and CsrC. Fold change shows the effects of DIP on specific CsrA, CsrB, and CsrC levels versus controls lacking DIP. Each experiment was repeated twice with essentially identical results. (A) RyhB sRNA response to DIP as a positive control for iron sequestration. (B) Purified C-terminally His_6-tagged CsrA protein served as a marker for the Western blotting. (A, C, and D) RNA isolated from strains deleted for *csrB* and for *csrC* is shown in the first and second lanes, respectively.

had no significant effect on growth of the WT strain under any condition (Fig. S2B to D). However, introduction of these knockouts into the *csrA* mutant led to partial or complete restoration of the WT growth rate in MOPS medium with limiting iron (Fig. 6E). In rich medium, the *csrA* mutant exhibited reduced growth only when iron was limiting, and this growth defect was completely recovered upon inactivation of *ftnB* alone; *dps* or *bfr* alone did not restore growth (Fig. 6B and C). Interestingly, the *csrA* mutant displayed a growth defect in the minimal medium under both iron conditions, although the effects were more pronounced in the iron-limited MOPS (Fig. 6D and E). Inactivation of *ftnB* in the *csrA* mutant recovered the growth rate completely in both iron-limited and iron-replete minimal media. The introduction of a *bfr* mutation to the *csrA* mutant partially restored growth in iron-replete and iron-limited MOPS (Fig. 6D and E). The *dps* mutation only improved growth of the *csrA* mutant in MOPS medium with limiting iron, and this effect was weak (Fig. 6D and E).

Iron availability has negligible effects on CsrA/B/C levels. A fundamental feature of Csr systems is their ability to integrate a variety of nutritional cues and signals and to interact with other regulators in diverse circuitry (10, 16, 29). Therefore, we sought to determine whether iron availability affects levels of Csr system components. Identically growing exponential-phase cultures of WT *E. coli* were treated with or without DIP (250 μM), and CsrA/B/C levels were measured. RyhB levels served as a positive control for the iron starvation response (Fig. 7A) (52). CsrA was determined by Western blotting using polyclonal anti-CsrA antibodies and normalized to RpoB (Fig. 7B). CsrA levels were unaffected by DIP addition, indicating that CsrA expression is not regulated in response to a change in iron availability. Northern blotting (Fig. 7C and D) showed that CsrB levels were unaffected by iron availability, although CsrC levels dropped slightly ~30 min after the addition of DIP. CsrB/C sRNAs function via CsrA, and CsrB is a more effective antagonist of CsrA than CsrC (56). Thus, the minor change in CsrC levels at 30 min might not have a significant impact on cellular physiology. In summary, it appears that iron availability has negligible effects on the key components of the Csr system and is not one of the cues to which the Csr system responds.

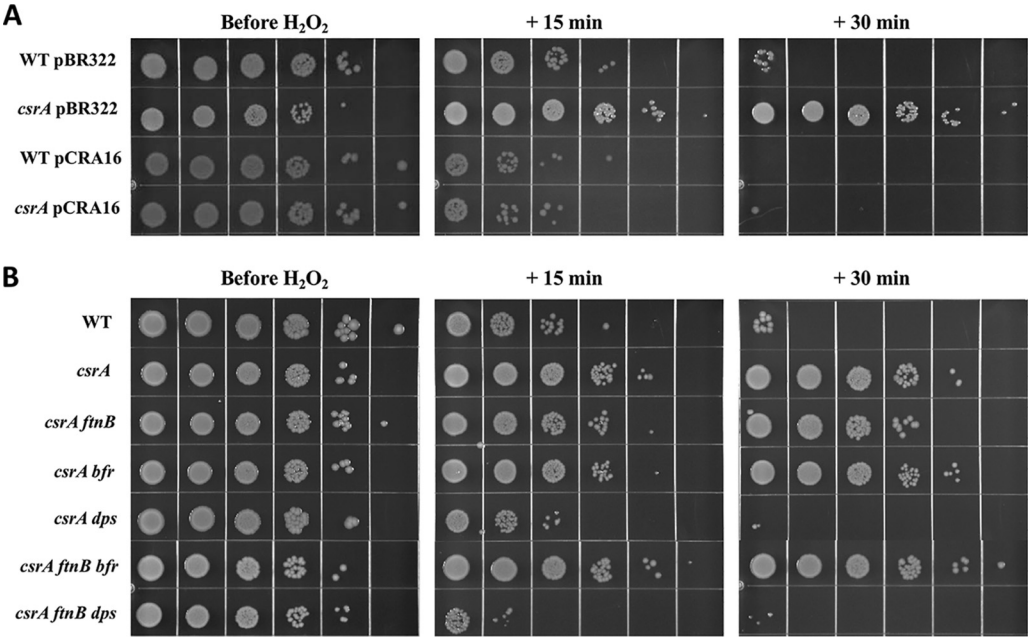

FIG 8 Survival of WT (MG1655) and *csrA* mutant strains upon exposure to H_2O_2. (A) WT and *csrA* mutant strains carrying pBR322 or plasmid pCRA16 (*csrA*$^+$). (B) WT, *csrA*, and *ftnB*, *dps*, and *bfr* combinatorial mutants. Strains were grown in LB to mid-exponential phase (OD_{600} of 0.5) and exposed to 12.5 mM H_2O_2. Samples were collected 0, 15, and 30 min after addition of H_2O_2, washed, and 10-fold serially diluted. The 10^{-1} to 10^{-6} dilutions were plated and grown for 18 h on LB agar at 37°C.

CsrA regulates resistance of *E. coli* against killing by H_2O_2. The finding that CsrA represses *sufA* (Fig. 1E), which encodes a protein involved in Fe-S assembly under oxidative stress (43), suggested that CsrA may play a role in regulating resistance against oxidative damage. To test this hypothesis, we exposed several isogenic strains to H_2O_2 during the exponential phase of growth and monitored its effect on viability. As suspected, the *csrA* mutant was considerably more resistant to oxidative stress than the WT strain (Fig. 8). Complementation restored sensitivity of the *csrA* mutant to H_2O_2, confirming a role for CsrA in repressing oxidative stress resistance. While deleting *ftnB* and/or *bfr* did not restore H_2O_2 sensitivity to the *csrA* mutant, the loss of *dps* caused a marked increase in H_2O_2 susceptibility, resulting in greater sensitivity even than in the *csrA* WT strain (Fig. 8B). Perhaps this is not surprising, given the importance of Dps in protection against oxidative stress (57). Finally, the WT and *csrA* mutant strains were tested for survival against H_2O_2 during early stationary phase. Unexpectedly, the *csrA* mutant was considerably more sensitive than WT to H_2O_2 at this stage of growth (see Fig. S3), opposite of its response in the exponential phase (Fig. 8). These observations are consistent with recent findings from *Salmonella enterica* that CsrA is a flexible regulator whose regulon varies under different growth or physiological conditions (58).

DISCUSSION

Here, we show that CsrA regulates at least 5 genes that participate in iron storage and utilization (Fig. 1). Repression of *ftnB* and *bfr* by CsrA affects cellular iron content (Fig. 5) and is required for optimal growth under iron limitation and in minimal medium (Fig. 6). In other words, repression of *ftnB* and *bfr* by CsrA positions the Csr system to guide intracellular iron flux toward growth-promoting processes. CsrA is known to broadly repress gene expression involved in stress responses and in the stationary phase of growth. Furthermore, the Csr system itself does not appear to respond to iron availability (Fig. 7). In contrast, CsrB and CsrC sRNAs are known to be expressed under conditions of stress or nutrient limitation, and by sequestering CsrA, these sRNAs diminish CsrA-mediated regulation of gene expression when growth is no longer a priority (4, 5, 30). This regulatory arrangement no doubt allows the cellular capacity for

iron storage to be governed in part by nutritional and growth phase conditions that influence the Csr system (29).

To our knowledge, the present studies represent the first evidence that the repression of gene expression by CsrA can be necessary for robust exponential growth, although modest growth support via CsrA-mediated repression has been observed (59). While the *csrA*::*gm* allele used in this study results in a much less severe growth defect than seen in a Δ*csrA* strain, even when the *csrA*::*gm* strain was grown under limiting iron conditions, we posit that the findings obtained with the *csrA*::*gm* mutant are nevertheless important for the following reasons. (i) Most likely, there is no environmental condition under which CsrA activity is absent, but there may be conditions under which reduced CsrA activity impacts iron requirements. (ii) In considering the development of CsrA inhibitors (60), complete inhibition of CsrA activity may not be required to achieve useful therapeutic effects, because human and animal body compartments tend to contain little available iron (see related discussion below).

The high-affinity binding of CsrA to *ftnB*, *dps*, and *bfr* transcripts (Fig. 3), taken together with *in vitro* translation results (Fig. 4A), indicates that CsrA represses translation of *ftnB*, *bfr*, and *dps* mRNAs by binding to the 5′ UTR of each transcript. Furthermore, RNase T1 footprinting revealed that CsrA binds to the *ftnB* SD sequence (Fig. 4B), which should directly impede ribosome loading. Translational repression of *hfq*, *glgC*, *cstA*, and *pgaA* expression is similarly mediated by CsrA binding to sites overlapping the SD sequences (21, 54, 61). Both *bfr* and *dps* transcripts contain potential CsrA binding sites overlapping their SD sequences (Fig. 3A), which might mediate translational repression by a similar mechanism (Fig. 4C).

The overexpression of *ftnB* and *bfr* in the *csrA* mutant caused excessive accumulation of cellular iron (Fig. 5). The *csrA* mutation also inhibited growth under iron-limiting conditions, apparently by altering iron bioavailability (Fig. 6). The relative magnitude of CsrA-dependent repression of genes for ISPs (*ftnB* > *bfr* > *dps*) mirrored the effects of these genes on cellular iron content and growth (*ftnB* > *bfr* > *dps*) (Fig. 1A to C, 5B, and 6C to E). We propose that during exponential growth, repression of the ISPs, particularly FtnB and Bfr, prevents the sequestration of iron away from iron-dependent growth processes. Importantly, the regulatory effects of CsrA on these genes became weaker or were eliminated as cultures entered the stationary phase of growth (Fig. 2), during which time *E. coli* becomes resistant to a variety of stressors (62).

The complex and dissimilar regulation of the *E. coli* ISPs seemingly complicates the interpretation of their individual physiological roles (34). *ftnA* expression is primarily regulated by Fur-mediated transcriptional activation, coupling FtnA levels to iron availability (63). At high iron levels, FtnA serves as the primary reservoir in *E. coli*, storing up to 50% of cellular iron (64). Under low to moderate iron levels, Bfr can become the principal ISP (65). Notably, *bfr* expression is induced by stresses, including osmotic and heat stress, while *ftnA* expression is not (66). Likewise, *ftnB* transcription can be driven by a σ^E-dependent promoter (67), linking FtnB production to extracytoplasmic stress, or from a σ^D-dependent promoter, as part of the Cpx regulon, connecting it to cell envelope damage (68). *dps* transcription is induced under oxidative stress by the transcriptional activator OxyR (69) and by σ^S during the stationary phase of growth (70). This regulatory diversity implies that individual ferritins are beneficial under different physiological conditions.

The strongest regulation by CsrA observed here was that of *ftnB* (Fig. 1A). FtnB is the major Fe^{2+} donor for the repair of oxidatively damaged Fe-sulfur clusters in *Salmonella*, although this is yet to be confirmed in *E. coli* (71). These findings raise the possibility that a primary role of CsrA in iron homeostasis is related to oxidative stress and repair response. CsrA also repressed *bfr* and *dps* (Fig. 1B and C), whose protein products appear to play modest roles in iron storage in *E. coli* and are linked to stress responses (64). CsrA repressed expression of *sufA* (Fig. 1E) and negatively affected the levels of *sufABCDE* operon transcripts (19), which encode proteins responsible for Fe-S cluster assembly under stress conditions. Recent research suggests that FtnB, Bfr, and Dps may each function to donate iron to the Suf Fe-S cluster biogenesis pathway (72). Thus, the

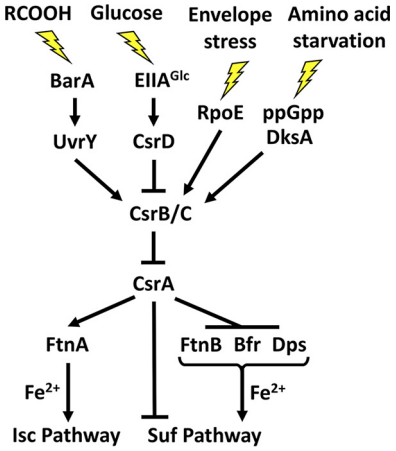

FIG 9 A model for regulation of iron homeostasis by CsrA in *E. coli*. During exponential growth and in the absence of stress, CsrA represses *ftnB*, *bfr*, *dps*, and *sufA*, inhibiting the delivery of iron to and the expression of the stress-resistant Suf Fe-S cluster assembly pathway. CsrA also activates the expression of *ftnA*, which donates iron to the Isc pathway. Upon stress or stationary-phase growth, CsrB/C sRNAs accumulate and sequester CsrA, which derepresses translation of *ftnB*, *bfr*, and *dps*, helping to divert iron from the housekeeping Isc Fe-S cluster assembly pathway and toward the Suf pathway. Activation of gene expression and iron transfer are indicated by arrows; repression is shown by a T bar.

present findings are consistent with a regulatory role of CsrA in the prevention and repair of oxidative damage.

CsrA modestly activated *ftnA* expression, in contrast to its stronger negative effects on the genes for the other ISPs. Unlike FtnB, Bfr, and Dps, FtnA does not appear to donate iron to the Suf Fe-S cluster biogenesis pathway (72). In fact, FtnA facilitates the assembly of iron-sulfur clusters via the Isc pathway under normal physiological conditions (73). Although Suf Fe-S biogenesis is preferred to Isc assembly during stress, the Suf pathway fails to fully mature some Fe-S proteins and may only meet the minimal Fe-S requirements for growth (43, 48, 74). As such, the activation of FtnA and repression of FtnB, Bfr, Dps, and SufA by CsrA may assist in directing iron stores toward the Fe-S assembly pathway that is most beneficial for exponential growth (Fig. 9). These findings suggest an explanation for the *csrA* growth defect in minimal medium, even when iron is replete. The loss of CsrA activation of FtnA and repression of FtnB, Bfr, Dps, and SufA apparently result in an inefficient utilization of available iron, which is particularly detrimental in minimal medium, where the demand for Fe-S proteins involved in biosynthetic processes may be high (75).

Interestingly, the ferritins are not the first example of CsrA mediating opposing regulatory effects on proteins having identical or highly related activities. For example, expression of the major phosphofructokinase, PfkA, is activated by CsrA, while the minor and σ^S-inducible enzyme, PfkB, is repressed by CsrA (1, 19, 76). The different allosteric responses of these enzymes to key metabolites are most likely the basis of their distinct regulatory patterns. To our knowledge, in such cases, CsrA consistently serves to repress the expression of genes associated with stationary-phase growth and/or stress responses, while tending to activate genes that are needed to support exponential growth.

The dramatically increased resistance of the *csrA* mutant to H_2O_2 during exponential growth demonstrates a regulatory role of CsrA in the resistance of *E. coli* to oxidative damage (Fig. 8). This is further supported by transcriptomics studies, which found increased steady-state mRNA levels for genes involved in antioxidant defense in the *csrA* mutant during exponential-phase growth, including the transcriptional activator of the superoxide response regulon, *soxS*, superoxide dismutases *sodA* and *sodC*, and catalase *katE* (19). CsrA also copurifies with mRNAs encoding the superoxide dismutase SodB and the catalase-peroxidase KatG (4). A recent study also provided evidence for a role for CsrA in repressing the oxidative stress response in *Salmonella* (58). The

repression of many genes involved in oxidative stress response pathways by CsrA suggests that ungoverned expression of these processes may be detrimental during exponential growth and in the absence of stress, when conditions favor high CsrA activity (30). Finally, the unexpected finding that the *csrA* mutant became less resistant than the WT to H_2O_2 in the stationary phase of growth (see Fig. S3 in the supplemental material) suggests that CsrA also performs important yet unexplained functions required for oxidative stress resistance in the stationary phase.

Commensal *E. coli* is ubiquitous in the gastrointestinal tracts of mammals and seemingly has colonized every mammalian species on the planet (77). While much research has been devoted to the role of CsrA in regulating virulence gene expression in pathogenic *Gammaproteobacteria* (10), little is known about its role in commensal colonization. *E. coli* inhabits the large intestine, which is primarily anoxic and nutrient limited. In this environment, soluble free iron is a contested and often limited resource (78). In addition, reactive oxygen species are scarce in the healthy intestinal lumen, although this can change during inflammation. For commensal microbes, iron is critical for enzyme function and energy generation. By repressing genes with the potential to sequester iron or divert iron to unnecessary stress response processes, CsrA fosters *E. coli* growth under iron-limiting laboratory conditions. We propose that it may play a similar role during colonization and survival in the large intestine.

MATERIALS AND METHODS

Bacterial strains and culture conditions. The bacterial strains and plasmids used in this study are listed in Table S2 in the supplemental material. All media and medium components were prepared using Nanopure water, 18.2 MΩ/cm (Barnstead). Bacterial strains were grown in LB broth (5 g yeast extract, 10 g Bacto tryptone, and 10 g NaCl per liter double-distilled water [ddH_2O]), pH 7.4, at 37°C, with shaking (250 rpm), unless otherwise indicated. For growth curves under iron-limiting and iron-replete conditions, MOPS defined medium (79) with 0.2% glucose was used; $FeSO_4$ was supplemented at the concentrations as indicated in the figure legends. L-Amino acid stock solutions were added to MOPS medium at the following final concentrations (mM): alanine (0.8), arginine (5.2), asparagine (0.4), aspartate (0.4), cysteine (0.1), glutamic acid (0.6), glutamine (0.6), glycine (0.8), histidine (0.2), isoleucine (0.4), leucine (0.8), lysine (0.4), methionine (0.2), phenylalanine (0.4), proline (0.4), serine (10.0), threonine (0.4), tryptophan (0.1), tyrosine (0.2), valine (0.6), and thiamine (0.01). When necessary, the following antibiotics were added to growth media: ampicillin (100 μg/ml), tetracycline (15 μg/ml), gentamicin (10 μg/ml), kanamycin (50 μg/ml), and chloramphenicol (25 μg/ml). Overnight cultures were routinely used to inoculate LB broth or minimal medium unless otherwise indicated. For strains carrying a *dps* deletion, exponentially growing cultures were used to prepare frozen glycerol stocks and to inoculate LB broth to eliminate/minimize the time spent under stationary-phase conditions.

Transduction with P1*vir* was used to introduce gene deletions and disruptions from *E. coli* donor strains constructed in previous studies (31, 80) and from the Keio library (81) (Table S2). Plasmids pBR322 (82) and pCRA16 (54) (*csrA* cloned into pBR322) were used in complementation tests. The Flp recombinase encoded in pCP20 (83) was used to eliminate the kanamycin resistance cassette, as required.

Considerations for strain construction. Because complete loss of CsrA activity causes severe growth defects and genetic instability (84, 85), our experiments were performed with strains carrying a mutation (*csrA*::*gm*) producing a protein that contains the first 50 of 61 amino acids of the native protein and has residual CsrA activity (31). This *csrA* allele can be transduced by selection for a distally encoded gentamicin resistance (*gm*) marker. Strains containing *fur csrA* double mutations produced copious biofilm, which interfered with growth and reporter assays (data not shown). CsrA represses *pgaABCD* expression, required for synthesis and secretion of the biofilm adhesin poly-β-1,6-*N*-acetyl-D-glucosamine (PGA) (54), and studies have also documented a role for Fur in biofilm formation (86, 87). Deletion of *pgaC*, encoding the PGA glycosyl transferase, abolished biofilm production by the strains in LB medium. Consequently, studies in LB were performed in the *pgaC* mutant background.

Construction of *′lacZ* reporter fusions. Chromosomal translational fusions to *′lacZ* were constructed using the CRIM system (88) and plasmid vector pLFT (4) and integrated at the λ*att* site. Single-copy integrants were confirmed by PCR, as described previously (88). Constructions were performed as follows: ~500 nucleotides (nt) of DNA upstream of and including the promoter region through one or more codons downstream of the translational start site was amplified by PCR using the associated primers (see Table S3). The PCR products were gel purified, digested with PstI and BamHI, ligated into PstI- and BamHI-digested and dephosphorylated plasmid pLFT, and electroporated into DH5α λpir cells. The fusion sequences were verified, and plasmids were isolated and integrated into the λ*att* site of strain MG1655 Δ*lacZ* using the helper plasmid pFINT (4).

β-Galactosidase assay. Strains containing *′lacZ* fusions were grown at 37°C in Luria-Bertani (LB) broth. Tetracycline (15 μg/ml) was used to ensure plasmid maintenance in strains bearing pBR322 or pCRA16. Cells were harvested at various times and β-galactosidase activity was measured as described previously (4). Total cell protein was measured following precipitation with 10% trichloroacetic acid,

using the bicinchoninic acid (BCA) assay (Pierce Biotechnology) with bovine serum albumin as the protein standard.

Electrophoretic gel mobility shift assays for RNA binding. The binding of CsrA to *ftnB*, *dps*, and *bfr* transcripts was determined by EMSA using *in vitro*-synthesized *ftnB*, *dps*, and *bfr* transcripts (MAXIscript SP6/MEGAshortscript T7 kits; Ambion) and recombinant CsrA-His_6 (14). The template DNAs for *in vitro* transcription of *ftnB* and *bfr* were generated by PCR from MG1655 genomic DNA, using oligonucleotide pairs *ftnB* SP6 fwd EMSA/*ftnB* SP6 rev EMSA and *bfr* T7 fwd EMSA/*bfr* T7 rev EMSA. The template DNA for *in vitro* transcription of *dps* was generated by annealing the oligonucleotide pair *dps* T7 EMSA/*dps* T7 EMSA comp. RNA was synthesized from the *ftnB* (127 nt, consisting of 127 nt of the 5′ UTR), *dps* (50 nt, consisting of 39 nt of the 5′ UTR and 11 nt of the coding region), and *bfr* (81 nt, consisting of the 23 nt 5′ UTR and 58 nt of the coding region) templates *in vitro* using the MEGAshortscript kit (Ambion). The resulting transcripts were purified via denaturing polyacrylamide gel electrophoresis (PAGE) followed by phenol-chloroform extraction and ethanol precipitation. Transcripts were treated with Antarctic phosphatase (NEB) and radiolabeled at the 5′ end using [γ-^{32}P]ATP and T4 polynucleotide kinase. Binding reaction mixtures contained 0.5 nM RNA, 10 mM $MgCl_2$, 100 mM KCl, 32.5 ng total yeast RNA, 20 mM dithiothreitol (DTT), 7.5% glycerol, 4 U SUPERasin (Ambion), and various concentrations of recombinant CsrA and were incubated at 37°C for 30 min. Reaction mixtures were separated on 9% native polyacrylamide gels (for *ftnB* mRNA) and 12% native polyacrylamide gels (for *dps* and *bfr* mRNAs) with 1× Tris-borate-EDTA (TBE) buffer. Competition assays were performed in the presence or absence of unlabeled specific (self) and nonspecific (*phoB*) RNA competitors using the minimum CsrA concentration required for a full shift. Labeled RNA was analyzed using a phosphorimager equipped with Quantity One software (Bio-Rad), as previously described (4). The apparent equilibrium binding constant (K_D) for CsrA-RNA complex formation was calculated according to a previously described cooperative binding equation (14).

Footprint assay. CsrA-*ftnB* RNA footprint assays were performed according to a published procedure (24). *ftnB* RNA (nt +1 to +152) was synthesized with the RNAMaxx kit (Agilent Technologies) using PCR-generated DNA templates. Gel-purified RNA was dephosphorylated and then 5′ end labeled using T4 polynucleotide kinase (New England BioLabs) and [γ-^{32}P]ATP (7,000 Ci/mmol). Labeled RNAs were renatured by heating for 1 min at 90°C followed by slow cooling to room temperature. Binding reaction mixtures (10 μl) contained 2 nM labeled RNA, 10 mM Tris-HCl (pH 7.5), 10 mM $MgCl_2$, 100 mM KCl, 40 ng of yeast RNA, 7.5% glycerol, 0.1 mg/ml xylene cyanol, and various concentrations of purified CsrA-His_6. After a 30-min incubation at 37°C to allow for CsrA-RNA complex formation, RNase T1 (0.016 U) was added and the incubation was continued for 15 min at 37°C. The reactions were stopped by adding 10 μl of stop solution (95% formamide, 0.025% SDS, 20 mM EDTA, 0.025% bromophenol blue, 0.025% xylene cyanol). Samples were heated for 5 min at 90°C and fractionated through standard 6% (vol/vol) polyacrylamide-8 M urea sequencing gels. Cleaved patterns were examined using a Typhoon 8600 variable mode imager.

Coupled transcription-translation assay. *In vitro* coupled transcription-translation assays using PURExpress (New England BioLabs) were performed according to a published procedure (89). Plasmid pYH333 contains a T7 promoter driving transcription of the *bfr* translational fusion (nt +1 to +50 relative to the *bfr* transcriptional start site). Plasmid pYH334 contains a T7 promoter driving transcription of the *dps* translational fusion (nt +1 to +81 relative to the *dps* transcriptional start site). Plasmid pYH336 contains a T7 promoter driving transcription of the *ftnB* translational fusion (nt +1 to +152 relative to the *ftnB* transcriptional start site). These plasmids were used as the templates for coupled transcription-translation reactions using the PURExpress *in vitro* protein synthesis kit, according to the manufacturer's instructions. Each 6.7-μl reaction mixture contained 250 ng of plasmid DNA template, various concentrations of purified CsrA-H_6, 1 U of RNasin (Promega), 2.5 mM DTT, 2.7 μl of solution A, and 2 μl of solution B. The mixtures were incubated for 2.5 h at 37°C, and β-galactosidase activity was determined according to the manufacturer's instructions.

Cellular iron measurement. Total cellular Fe concentrations were measured by inductively coupled plasma optical emission spectrometry (ICP-OES) at the University of Florida Institute of Food and Agricultural Sciences Analytical Services Laboratories. LB medium (500 ml) was inoculated with overnight cultures and incubated at 37°C with shaking. Two hundred fifty milliliters of exponential-phase cultures (OD_{600} of 0.5) were harvested by centrifugation and washed three times in cold phosphate-buffered saline (PBS). The resulting bacterial pellets were resuspended in 1 ml 35% HNO_3 (trace-metal grade) treated at 95°C and diluted 1:10 with Invitrogen UltraPure distilled water. Fe concentrations were normalized to total protein. For quantification of iron in the medium, 2 ml trace-metal-grade 35% HNO_3 was added to 18 ml medium for ICP-OES analysis. Glassware for these experiments was pretreated overnight to remove trace metal contamination with 20% trace-metal-grade HNO_3 and multiple rinses with Nanopure water.

Growth kinetics assay. Growth under Fe-limiting and -replete conditions was monitored by OD_{600} measurements in MOPS minimal medium (see "Bacterial strains and culture conditions") or by BCA protein assay in Luria-Bertani (LB) medium. All medium components were filter sterilized. Prior to use, labware was treated overnight in a 20% trace-metal-grade HNO_3 and rinsed multiple times with Nanopure water. ICP-OES analysis indicated that final Fe concentration of the MOPS medium before Fe supplementation was below 0.01 μM. For growth experiments performed in MOPS, overnight cultures were grown in MOPS with 0.05 μM $FeSO_4$ and were diluted 1:100 (except for cultures carrying the *dps* mutation, which were inoculated directly from −80°C glycerol stocks) and grown to exponential phase in MOPS with 0.05 or 100 μM $FeSO_4$. Growth experiments in LB were started from overnight cultures in LB, which were diluted 1:100 and grown to exponential phase in LB. The growth curves in all media were

started at an OD_{600} of 0.01 from the exponentially growing cultures. Total cell protein was measured following precipitation with 10% trichloroacetic acid, using the BCA assay (Pierce Biotechnology) with bovine serum albumin as the protein standard. The growth rate constant (μ) was calculated from the exponential phase of growth: $\mu = 2.303(\log OD_2 - \log OD_1)/(t_2 - t_1)$.

Western blotting of CsrA and FecB-3×FLAG protein. Samples for CsrA immunoblotting were harvested at intervals after the addition of 250 μM iron chelator 2,2′-dipyridyl. Samples for FecB-3×FLAG blots were harvested at an OD_{600} of 0.05 from LB supplemented with 1 mM sodium citrate to induce expression. Cells were centrifuged and resuspended in 2× sample buffer (4% [wt/vol] SDS, 0.16 M Tris, 1.5% [vol/vol] β-mercaptoethanol, 20% [vol/vol] glycerol, 0.02% [wt/vol] bromophenol blue, pH 6.0), normalized by the OD, and lysed by sonication and boiling. Samples were separated by SDS-PAGE, transferred to 0.2 μM polyvinylidene difluoride (PVDF) membranes, and detected using polyclonal anti-CsrA or monoclonal anti-FLAG for FecB-3×FLAG, or anti-RpoB antibodies, as described previously (90).

Northern blotting. Samples were harvested and total cellular RNA was isolated using the RNeasy minikit (Qiagen). Total RNA was mixed with 2 volumes of loading buffer (50% [vol/vol] deionized formamide, 6% [vol/vol] formaldehyde, 1× MOPS [20 mM], 5 mM sodium acetate [NaOAc], 2 mM EDTA [pH 7.0], 10% [vol/vol] glycerol, 0.05% [wt/vol] bromophenol blue, 0.01% [wt/vol] ethidium bromide), denatured by heating at 95°C for 5 min, placed on ice, and separated by electrophoresis on a 7 M urea-5% polyacrylamide gel. RNA was transferred and fixed to a positively charged nylon membrane (Roche) and hybridized with digoxigenin (DIG)-labeled antisense CsrB, CsrC, or RyhB RNA probes as previously described (5). Transferred rRNA served as a loading control and was stained with methylene blue, imaged using a Gel-Doc, and signal intensity was quantified using Quantity One software. CsrB or CsrC RNAs signals were captured with a ChemiDoc XRS+ system (Bio-Rad, Hercules, CA).

Oxidative stress assay. WT and mutant strains were grown in LB to mid-exponential (OD_{600} of 0.5) or early stationary (OD_{600} of 2.5) phase and exposed to H_2O_2 (12.5 mM and 50.0 mM, respectively). After 0, 15, and 30 min, samples were collected, washed 3 times in pH 7.4 PBS, and 10-fold serially diluted. Cells were plated on LB and grown for 18 h at 37°C before imaging the resulting colonies.

SUPPLEMENTAL MATERIAL

Supplemental material for this article may be found at https://doi.org/10.1128/mBio.01034-19.

FIG S1, TIF file, 2.9 MB.

FIG S2, TIF file, 2.9 MB.

FIG S3, TIF file, 2.2 MB.

TABLE S1, DOCX file, 0.1 MB.

TABLE S2, DOCX file, 0.1 MB.

TABLE S3, DOCX file, 0.1 MB.

ACKNOWLEDGMENTS

This project was funded by NIH R01 grant GM059969 to Tony Romeo and Paul Babitzke and by the National Science Foundation Graduate Research Fellowship Program (DGE-1315138 to Anastasia Potts).

The funders had no role in study design, data collection and analysis, decision to publish, or preparation of the manuscript.

REFERENCES

1. Sabnis NA, Yang H, Romeo T. 1995. Pleiotropic regulation of central carbohydrate metabolism in *Escherichia coli* via the gene *csrA*. J Biol Chem 270:29096–29104. https://doi.org/10.1074/jbc.270.49.29096.
2. Morin M, Ropers D, Letisse F, Laguerre S, Portais JC, Cocaign-Bousquet M, Enjalbert B. 2016. The post-transcriptional regulatory system CSR controls the balance of metabolic pools in upper glycolysis of *Escherichia coli*. Mol Microbiol 100:686–700. https://doi.org/10.1111/mmi.13343.
3. Revelles O, Millard P, Nougayrède JP, Dobrindt U, Oswald E, Létisse F, Portais JC. 2013. The carbon storage regulator (Csr) system exerts a nutrient-specific control over central metabolism in *Escherichia coli* strain Nissle 1917. PLoS One 8:e66386. https://doi.org/10.1371/journal.pone.0066386.
4. Edwards AN, Patterson-Fortin LM, Vakulskas CA, Mercante JW, Potrykus K, Vinella D, Camacho MI, Fields JA, Thompson SA, Georgellis D, Cashel M, Babitzke P, Romeo T. 2011. Circuitry linking the Csr and stringent response global regulatory systems. Mol Microbiol 80:1561–1580. https://doi.org/10.1111/j.1365-2958.2011.07663.x.
5. Pannuri A, Vakulskas CA, Zere T, McGibbon LC, Edwards AN, Georgellis D, Babitzke P, Romeo T. 2016. Circuitry linking the catabolite repression and Csr global regulatory systems of *Escherichia coli*. J Bacteriol 198:3000–3015. https://doi.org/10.1128/JB.00454-16.
6. Yakhnin H, Aichele R, Ades SE, Romeo T, Babitzke P. 2017. Circuitry linking the global Csr and σ^E-dependent cell envelope stress response systems. J Bacteriol 199:e00484-17. https://doi.org/10.1128/JB.00484-17.
7. Jackson DW, Suzuki K, Oakford L, Simecka JW, Hart ME, Romeo T. 2002. Biofilm formation and dispersal under the influence of the global regulator CsrA of *Escherichia coli*. J Bacteriol 184:290–301. https://doi.org/10.1128/jb.184.1.290-301.2002.
8. Wei BL, Brun-Zinkernagel AM, Simecka JW, Prüss BM, Babitzke P, Romeo T. 2001. Positive regulation of motility and *flhDC* expression by the RNA-binding protein CsrA of *Escherichia coli*. Mol Microbiol 40:245–256. https://doi.org/10.1046/j.1365-2958.2001.02380.x.
9. Yakhnin H, Baker CS, Berezin I, Evangelista MA, Rassin A, Romeo T, Babitzke P. 2011. CsrA represses translation of *sdiA*, which encodes the *N*-acylhomoserine-L-lactone receptor of *Escherichia coli*, by binding exclusively within the coding region of *sdiA* mRNA. J Bacteriol 193:6162–6170. https://doi.org/10.1128/JB.05975-11.
10. Vakulskas CA, Potts AH, Babitzke P, Ahmer BM, Romeo T. 2015. Regula-

tion of bacterial virulence by Csr (Rsm) systems. Microbiol Mol Biol Rev 79:193–224. https://doi.org/10.1128/MMBR.00052-14.
11. White D, Hart ME, Romeo T. 1996. Phylogenetic distribution of the global regulatory gene *csrA* among eubacteria. Gene 182:221–223. https://doi.org/10.1016/s0378-1119(96)00547-1.
12. Zere TR, Vakulskas CA, Leng Y, Pannuri A, Potts AH, Dias R, Tang D, Kolaczkowski B, Georgellis D, Ahmer BM, Romeo T. 2015. Genomic targets and features of BarA-UvrY (-SirA) signal transduction systems. PLoS One 10:e0145035. https://doi.org/10.1371/journal.pone.0145035.
13. Romeo T, Gong M, Liu MY, Brun-Zinkernagel AM. 1993. Identification and molecular characterization of *csrA*, a pleiotropic gene from *Escherichia coli* that affects glycogen biosynthesis, gluconeogenesis, cell size, and surface properties. J Bacteriol 175:4744–4755. https://doi.org/10.1128/jb.175.15.4744-4755.1993.
14. Mercante J, Suzuki K, Cheng X, Babitzke P, Romeo T. 2006. Comprehensive alanine-scanning mutagenesis of *Escherichia coli* CsrA defines two subdomains of critical functional importance. J Biol Chem 281:31832–31842. https://doi.org/10.1074/jbc.M606057200.
15. Schubert M, Lapouge K, Duss O, Oberstrass FC, Jelesarov I, Haas D, Allain FH. 2007. Molecular basis of messenger RNA recognition by the specific bacterial repressing clamp RsmA/CsrA. Nat Struct Mol Biol 14:807–813. https://doi.org/10.1038/nsmb1285.
16. Romeo T, Vakulskas CA, Babitzke P. 2013. Post-transcriptional regulation on a global scale: form and function of Csr/Rsm systems. Environ Microbiol 15:313–324. https://doi.org/10.1111/j.1462-2920.2012.02794.x.
17. Romeo T. 1998. Global regulation by the small RNA-binding protein CsrA and the non-coding RNA molecule CsrB. Mol Microbiol 29:1321–1330. https://doi.org/10.1046/j.1365-2958.1998.01021.x.
18. Dubey AK, Baker CS, Romeo T, Babitzke P. 2005. RNA sequence and secondary structure participate in high-affinity CsrA-RNA interaction. RNA 11:1579–1587. https://doi.org/10.1261/rna.2990205.
19. Potts AH, Vakulskas CA, Pannuri A, Yakhnin H, Babitzke P, Romeo T. 2017. Global role of the bacterial post-transcriptional regulator CsrA revealed by integrated transcriptomics. Nat Commun 8:1596. https://doi.org/10.1038/s41467-017-01613-1.
20. Yakhnin H, Pandit P, Petty TJ, Baker CS, Romeo T, Babitzke P. 2007. CsrA of *Bacillus subtilis* regulates translation initiation of the gene encoding the flagellin protein (*hag*) by blocking ribosome binding. Mol Microbiol 64:1605–1620. https://doi.org/10.1111/j.1365-2958.2007.05765.x.
21. Baker CS, Eory LA, Yakhnin H, Mercante J, Romeo T, Babitzke P. 2007. CsrA inhibits translation initiation of *Escherichia coli hfq* by binding to a single site overlapping the Shine-Dalgarno sequence. J Bacteriol 189:5472–5481. https://doi.org/10.1128/JB.00529-07.
22. Patterson-Fortin LM, Vakulskas CA, Yakhnin H, Babitzke P, Romeo T. 2013. Dual posttranscriptional regulation via a cofactor-responsive mRNA leader. J Mol Biol 425:3662–3677. https://doi.org/10.1016/j.jmb.2012.12.010.
23. Irie Y, Starkey M, Edwards AN, Wozniak DJ, Romeo T, Parsek MR. 2010. *Pseudomonas aeruginosa* biofilm matrix polysaccharide Psl is regulated transcriptionally by RpoS and post-transcriptionally by RsmA. Mol Microbiol 78:158–172. https://doi.org/10.1111/j.1365-2958.2010.07320.x.
24. Yakhnin AV, Baker CS, Vakulskas CA, Yakhnin H, Berezin I, Romeo T, Babitzke P. 2013. CsrA activates *flhDC* expression by protecting *flhDC* mRNA from RNase E-mediated cleavage. Mol Microbiol 87:851–866. https://doi.org/10.1111/mmi.12136.
25. Figueroa-Bossi N, Schwartz A, Guillemardet B, D'Heygère F, Bossi L, Boudvillain M. 2014. RNA remodeling by bacterial global regulator CsrA promotes Rho-dependent transcription termination. Genes Dev 28:1239–1251. https://doi.org/10.1101/gad.240192.114.
26. Yakhnin H, Yakhnin AV, Baker CS, Sineva E, Berezin I, Romeo T, Babitzke P. 2011. Complex regulation of the global regulatory gene *csrA*: CsrA-mediated translational repression, transcription from five promoters by $E\sigma^{70}$ and $E\sigma^{S}$, and indirect transcriptional activation by CsrA. Mol Microbiol 81:689–704. https://doi.org/10.1111/j.1365-2958.2011.07723.x.
27. Babitzke P, Romeo T. 2007. CsrB sRNA family: sequestration of RNA-binding regulatory proteins. Curr Opin Microbiol 10:156–163. https://doi.org/10.1016/j.mib.2007.03.007.
28. Chavez RG, Alvarez AF, Romeo T, Georgellis D. 2010. The physiological stimulus for the BarA sensor kinase. J Bacteriol 192:2009–2012. https://doi.org/10.1128/JB.01685-09.
29. Romeo T, Babitzke P. 2018. Global regulation by CsrA and its RNA antagonists. Microbiol Spectr 6:RWR-0009-2017. https://doi.org/10.1128/microbiolspec.RWR-0009-2017.
30. Leng Y, Vakulskas CA, Zere TR, Pickering BS, Watnick PI, Babitzke P, Romeo T. 2016. Regulation of CsrB/C sRNA decay by $EIIA^{Glc}$ of the phosphoenolpyruvate: carbohydrate phosphotransferase system. Mol Microbiol 99:627–639. https://doi.org/10.1111/mmi.13259.
31. Vakulskas CA, Leng Y, Abe H, Amaki T, Okayama A, Babitzke P, Suzuki K, Romeo T. 2016. Antagonistic control of the turnover pathway for the global regulatory sRNA CsrB by the CsrA and CsrD proteins. Nucleic Acids Res 44:7896–7910. https://doi.org/10.1093/nar/gkw484.
32. Darnell RB. 2010. HITS-CLIP: panoramic views of protein-RNA regulation in living cells. Wiley Interdiscip Rev RNA 1:266–286. https://doi.org/10.1002/wrna.31.
33. Wheeler EC, Van Nostrand EL, Yeo GW. 2018. Advances and challenges in the detection of transcriptome-wide protein-RNA interactions. Wiley Interdiscip Rev RNA 9:e1436. https://doi.org/10.1002/wrna.1436.
34. Andrews SC, Robinson AK, Rodríguez-Quiñones F. 2003. Bacterial iron homeostasis. FEMS Microbiol Rev 27:215–237. https://doi.org/10.1016/S0168-6445(03)00055-X.
35. Andrews S, Norton I, Salunkhe AS, Goodluck H, Aly WS, Mourad-Agha H, Cornelis P. 2013. Control of iron metabolism in bacteria. Met Ions Life Sci 12:203–239. https://doi.org/10.1007/978-94-007-5561-1_7.
36. Salvail H, Massé E. 2012. Regulating iron storage and metabolism with RNA: an overview of posttranscriptional controls of intracellular iron homeostasis. Wiley Interdiscip Rev RNA 3:26–36. https://doi.org/10.1002/wrna.102.
37. Braun V. 2001. Iron uptake mechanisms and their regulation in pathogenic bacteria. Int J Med Microbiol 291:67–79. https://doi.org/10.1078/1438-4221-00103.
38. Skaar EP. 2010. The battle for iron between bacterial pathogens and their vertebrate hosts. PLoS Pathog 6:e1000949. https://doi.org/10.1371/journal.ppat.1000949.
39. Frawley ER, Fang FC. 2014. The ins and outs of bacterial iron metabolism. Mol Microbiol 93:609–616. https://doi.org/10.1111/mmi.12709.
40. Porcheron G, Dozois CM. 2015. Interplay between iron homeostasis and virulence: Fur and RyhB as major regulators of bacterial pathogenicity. Vet Microbiol 179:2–14. https://doi.org/10.1016/j.vetmic.2015.03.024.
41. Lill R. 2009. Function and biogenesis of iron-sulphur proteins. Nature 460:831–838. https://doi.org/10.1038/nature08301.
42. Roche B, Aussel L, Ezraty B, Mandin P, Py B, Barras F. 2013. Iron/sulfur proteins biogenesis in prokaryotes: formation, regulation and diversity. Biochim Biophys Acta 1827:455–469. https://doi.org/10.1016/j.bbabio.2012.12.010.
43. Mettert EL, Kiley PJ. 2015. How is Fe-S cluster formation regulated? Annu Rev Microbiol 69:505–526. https://doi.org/10.1146/annurev-micro-091014-104457.
44. Jang S, Imlay JA. 2010. Hydrogen peroxide inactivates the *Escherichia coli* Isc iron-sulphur assembly system, and OxyR induces the Suf system to compensate. Mol Microbiol 78:1448–1467. https://doi.org/10.1111/j.1365-2958.2010.07418.x.
45. Outten FW, Djaman O, Storz G. 2004. A *suf* operon requirement for Fe-S cluster assembly during iron starvation in *Escherichia coli*. Mol Microbiol 52:861–872. https://doi.org/10.1111/j.1365-2958.2004.04025.x.
46. Justino MC, Vicente JB, Teixeira M, Saraiva LM. 2005. New genes implicated in the protection of anaerobically grown *Escherichia coli* against nitric oxide. J Biol Chem 280:2636–2643. https://doi.org/10.1074/jbc.M411070200.
47. Dai Y, Outten FW. 2012. The *E. coli* SufS-SufE sulfur transfer system is more resistant to oxidative stress than IscS-IscU. FEBS Lett 586:4016–4022. https://doi.org/10.1016/j.febslet.2012.10.001.
48. Mettert EL, Kiley PJ. 2014. Coordinate regulation of the Suf and Isc Fe-S cluster biogenesis pathways by IscR is essential for viability of *Escherichia coli*. J Bacteriol 196:4315–4323. https://doi.org/10.1128/JB.01975-14.
49. Fillat MF. 2014. The FUR (ferric uptake regulator) superfamily: diversity and versatility of key transcriptional regulators. Arch Biochem Biophys 546:41–52. https://doi.org/10.1016/j.abb.2014.01.029.
50. Jacques JF, Jang S, Prévost K, Desnoyers G, Desmarais M, Imlay J, Massé E. 2006. RyhB small RNA modulates the free intracellular iron pool and is essential for normal growth during iron limitation in *Escherichia coli*. Mol Microbiol 62:1181–1190. https://doi.org/10.1111/j.1365-2958.2006.05439.x.
51. Kulkarni PR, Jia T, Kuehne SA, Kerkering TM, Morris ER, Searle MS, Heeb S, Rao J, Kulkarni RV. 2014. A sequence-based approach for prediction of CsrA/RsmA targets in bacteria with experimental validation in *Pseudomonas aeruginosa*. Nucleic Acids Res 42:6811–6825. https://doi.org/10.1093/nar/gku309.
52. Massé E, Gottesman S. 2002. A small RNA regulates the expression of

genes involved in iron metabolism in *Escherichia coli*. Proc Natl Acad Sci U S A 99:4620–4625. https://doi.org/10.1073/pnas.032066599.
53. Grainger DC, Goldberg MD, Lee DJ, Busby SJ. 2008. Selective repression by Fis and H-NS at the *Escherichia coli dps* promoter. Mol Microbiol 68:1366–1377. https://doi.org/10.1111/j.1365-2958.2008.06253.x.
54. Wang X, Dubey AK, Suzuki K, Baker CS, Babitzke P, Romeo T. 2005. CsrA post-transcriptionally represses *pgaABCD*, responsible for synthesis of a biofilm polysaccharide adhesin of *Escherichia coli*. Mol Microbiol 56:1648–1663. https://doi.org/10.1111/j.1365-2958.2005.04648.x.
55. Hartmann A, Braun V. 1981. Iron uptake and iron limited growth of *Escherichia coli* K-12. Arch Microbiol 130:353–356. https://doi.org/10.1007/BF00414599.
56. Weilbacher T, Suzuki K, Dubey AK, Wang X, Gudapaty S, Morozov I, Baker CS, Georgellis D, Babitzke P, Romeo T. 2003. A novel sRNA component of the carbon storage regulatory system of *Escherichia coli*. Mol Microbiol 48:657–670. https://doi.org/10.1046/j.1365-2958.2003.03459.x.
57. Calhoun LN, Kwon YM. 2011. Structure, function and regulation of the DNA-binding protein Dps and its role in acid and oxidative stress resistance in *Escherichia coli*: a review. J Appl Microbiol 110:375–386. https://doi.org/10.1111/j.1365-2672.2010.04890.x.
58. Potts AH, Guo Y, Ahmer BMM, Romeo T. 2019. Role of CsrA in stress responses and metabolism important for *Salmonella* virulence revealed by integrated transcriptomics. PLoS One 14:e0211430. https://doi.org/10.1371/journal.pone.0211430.
59. Morin M, Ropers D, Cinquemani E, Portais JC, Enjalbert B, Cocaign-Bousquet M. 2017. The Csr system regulates *Escherichia coli* fitness by controlling glycogen accumulation and energy levels. mBio 8:e01628-17. https://doi.org/10.1128/mBio.01628-17.
60. Maurer CK, Fruth M, Empting M, Avrutina O, Hoßmann J, Nadmid S, Gorges J, Herrmann J, Kazmaier U, Dersch P, Müller R, Hartmann RW. 2016. Discovery of the first small-molecule CsrA-RNA interaction inhibitors using biophysical screening technologies. Future Med Chem 8:931–947. https://doi.org/10.4155/fmc-2016-0033.
61. Dubey AK, Baker CS, Suzuki K, Jones AD, Pandit P, Romeo T, Babitzke P. 2003. CsrA regulates translation of the *Escherichia coli* carbon starvation gene, *cstA*, by blocking ribosome access to the *cstA* transcript. J Bacteriol 185:4450–4460. https://doi.org/10.1128/jb.185.15.4450-4460.2003.
62. Battesti A, Majdalani N, Gottesman S. 2011. The RpoS-mediated general stress response in *Escherichia coli*. Annu Rev Microbiol 65:189–213. https://doi.org/10.1146/annurev-micro-090110-102946.
63. Nandal A, Huggins CC, Woodhall MR, McHugh J, Rodríguez-Quiñones F, Quail MA, Guest JR, Andrews SC. 2010. Induction of the ferritin gene (*ftnA*) of *Escherichia coli* by Fe^{2+}-Fur is mediated by reversal of H-NS silencing and is RyhB independent. Mol Microbiol 75:637–657. https://doi.org/10.1111/j.1365-2958.2009.06977.x.
64. Abdul-Tehrani H, Hudson AJ, Chang YS, Timms AR, Hawkins C, Williams JM, Harrison PM, Guest JR, Andrews SC. 1999. Ferritin mutants of *Escherichia coli* are iron deficient and growth impaired, and *fur* mutants are iron deficient. J Bacteriol 181:1415–1428.
65. Outten W, Rouault T (ed). 2014. Iron-sulfur clusters in chemistry and biology. Walter de Gruyter GmbH, Berlin, Germany.
66. Gunasekera TS, Csonka LN, Paliy O. 2008. Genome-wide transcriptional responses of *Escherichia coli* K-12 to continuous osmotic and heat stresses. J Bacteriol 190:3712–3720. https://doi.org/10.1128/JB.01990-07.
67. Rhodius VA, Suh WC, Nonaka G, West J, Gross CA. 2006. Conserved and variable functions of the σ^E stress response in related genomes. PLoS Biol 4:e2. https://doi.org/10.1371/journal.pbio.0040002.
68. Yamamoto K, Ishihama A. 2006. Characterization of copper-inducible promoters regulated by CpxA/CpxR in *Escherichia coli*. Biosci Biotechnol Biochem 70:1688–1695. https://doi.org/10.1271/bbb.60024.
69. Altuvia S, Almirón M, Huisman G, Kolter R, Storz G. 1994. The *dps* promoter is activated by OxyR during growth and by IHF and σS in stationary phase. Mol Microbiol 13:265–272. https://doi.org/10.1111/j.1365-2958.1994.tb00421.x.
70. Singh SS, Typas A, Hengge R, Grainger DC. 2011. *Escherichia coli* σ^{70} senses sequence and conformation of the promoter spacer region. Nucleic Acids Res 39:5109–5118. https://doi.org/10.1093/nar/gkr080.
71. Velayudhan J, Castor M, Richardson A, Main-Hester KL, Fang FC. 2007. The role of ferritins in the physiology of *Salmonella enterica* sv. Typhimurium: a unique role for ferritin B in iron-sulphur cluster repair and virulence. Mol Microbiol 63:1495–1507. https://doi.org/10.1111/j.1365-2958.2007.05600.x.
72. Bolaji N. 2017. Characterization of the SUF FE-S pathway in *Escherichia coli*. University of South Carolina, Columbia, SC.
73. Bitoun JP, Wu G, Ding H. 2008. *Escherichia coli* FtnA acts as an iron buffer for re-assembly of iron-sulfur clusters in response to hydrogen peroxide stress. Biometals 21:693–703. https://doi.org/10.1007/s10534-008-9154-7.
74. Ezraty B, Vergnes A, Banzhaf M, Duverger Y, Huguenot A, Brochado AR, Su SY, Espinosa L, Loiseau L, Py B, Typas A, Barras F. 2013. Fe-S cluster biosynthesis controls uptake of aminoglycosides in a ROS-less death pathway. Science 340:1583–1587. https://doi.org/10.1126/science.1238328.
75. Tao H, Bausch C, Richmond C, Blattner FR, Conway T. 1999. Functional genomics: expression analysis of *Escherichia coli* growing on minimal and rich media. J Bacteriol 181:6425–6440.
76. Lacour S, Landini P. 2004. σ^S-dependent gene expression at the onset of stationary phase in *Escherichia coli*: function of σS-dependent genes and identification of their promoter sequences. J Bacteriol 186:7186–7195. https://doi.org/10.1128/JB.186.21.7186-7195.2004.
77. Conway T, Cohen PS. 2015. Commensal and pathogenic *Escherichia coli* metabolism in the gut. Microbiol Spectr 3:MBP-0006-2014. https://doi.org/10.1128/microbiolspec.MBP-0006-2014.
78. Kortman GA, Raffatellu M, Swinkels DW, Tjalsma H. 2014. Nutritional iron turned inside out: intestinal stress from a gut microbial perspective. FEMS Microbiol Rev 38:1202–1234. https://doi.org/10.1111/1574-6976.12086.
79. Neidhardt FC, Bloch PL, Smith DF. 1974. Culture medium for enterobacteria. J Bacteriol 119:736–747.
80. Wang X, Preston JF, Romeo T. 2004. The *pgaABCD* locus of *Escherichia coli* promotes the synthesis of a polysaccharide adhesin required for biofilm formation. J Bacteriol 186:2724–2734. https://doi.org/10.1128/jb.186.9.2724-2734.2004.
81. Baba T, Ara T, Hasegawa M, Takai Y, Okumura Y, Baba M, Datsenko KA, Tomita M, Wanner BL, Mori H. 2006. Construction of *Escherichia coli* K-12 in-frame, single-gene knockout mutants: the Keio collection. Mol Syst Biol 2:2006.0008. https://doi.org/10.1038/msb4100050.
82. Bolivar F, Rodriguez RL, Greene PJ, Betlach MC, Heyneker HL, Boyer HW, Crosa JH, Falkow S. 1977. Construction and characterization of new cloning vehicles. II. A multipurpose cloning system. Gene 2:95–113. https://doi.org/10.1016/0378-1119(77)90000-2.
83. Cherepanov PP, Wackernagel W. 1995. Gene disruption in *Escherichia coli*: TcR and KmR cassettes with the option of Flp-catalyzed excision of the antibiotic-resistance determinant. Gene 158:9–14. https://doi.org/10.1016/0378-1119(95)00193-a.
84. Timmermans J, Van Melderen L. 2009. Conditional essentiality of the *csrA* gene in *Escherichia coli*. J Bacteriol 191:1722–1724. https://doi.org/10.1128/JB.01573-08.
85. Lawhon SD, Frye JG, Suyemoto M, Porwollik S, McClelland M, Altier C. 2003. Global regulation by CsrA in *Salmonella typhimurium*. Mol Microbiol 48:1633–1645. https://doi.org/10.1046/j.1365-2958.2003.03535.x.
86. Kurabayashi K, Agata T, Asano H, Tomita H, Hirakawa H. 2016. Fur represses adhesion to, invasion of, and intracellular bacterial community formation within bladder epithelial cells and motility in Uropathogenic *Escherichia coli*. Infect Immun 84:3220–3231. https://doi.org/10.1128/IAI.00369-16.
87. Magistro G, Hoffmann C, Schubert S. 2015. The salmochelin receptor IroN itself, but not salmochelin-mediated iron uptake promotes biofilm formation in extraintestinal pathogenic *Escherichia coli* (ExPEC). Int J Med Microbiol 305:435–445. https://doi.org/10.1016/j.ijmm.2015.03.008.
88. Haldimann A, Wanner BL. 2001. Conditional-replication, integration, excision, and retrieval plasmid-host systems for gene structure-function studies of bacteria. J Bacteriol 183:6384–6393. https://doi.org/10.1128/JB.183.21.6384-6393.2001.
89. Park H, Yakhnin H, Connolly M, Romeo T, Babitzke P. 2015. CsrA participates in a PNPase autoregulatory mechanism by selectively repressing translation of *pnp* transcripts that have been previously processed by RNase III and PNPase. J Bacteriol 197:3751–3759. https://doi.org/10.1128/JB.00721-15.
90. Vakulskas CA, Pannuri A, Cortés-Selva D, Zere TR, Ahmer BM, Babitzke P, Romeo T. 2014. Global effects of the DEAD-box RNA helicase DeaD (CsdA) on gene expression over a broad range of temperatures. Mol Microbiol 92:945–958. https://doi.org/10.1111/mmi.12606.